Biological Interfaces

requirements in nature

protection & defense

anti-wetting

transport

aerodynamics

acoustics

sensors

optics

adhesion enhancement or reductions

defense

occurrence of cuticle microstructures (CMS),
hydrophobic property (HP),
appearance of integument (IA)

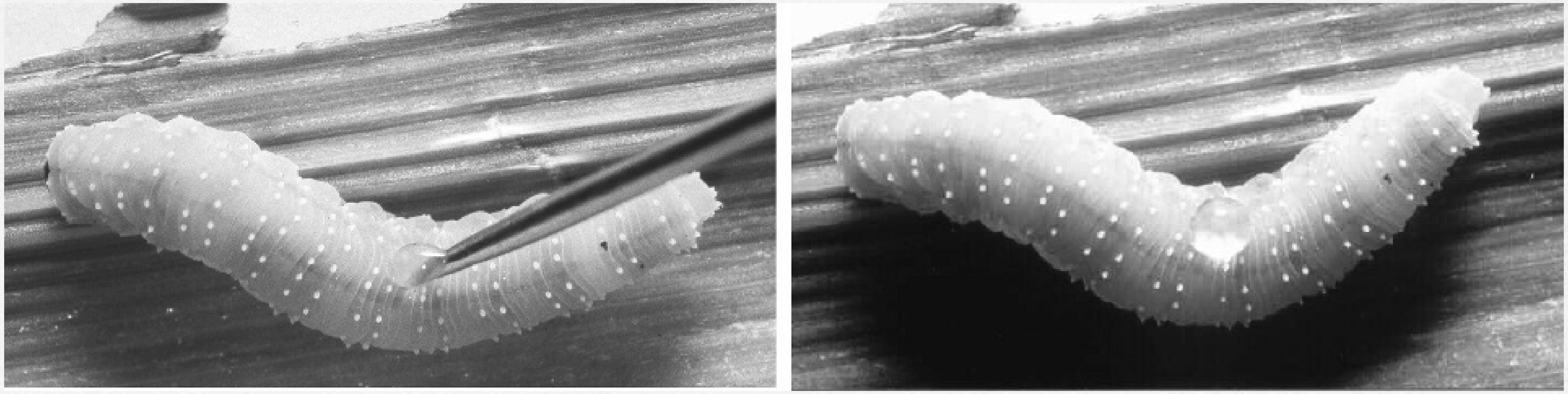

Fig. 2.1 The easy bleeding phenomenon. A larva of *Rhadinoceraea micans*, approximately 15–17 mm in length, is slightly touched on its body with a needle (*left*). A hemolymph droplet immediately appears at this spot (*right*)

defense

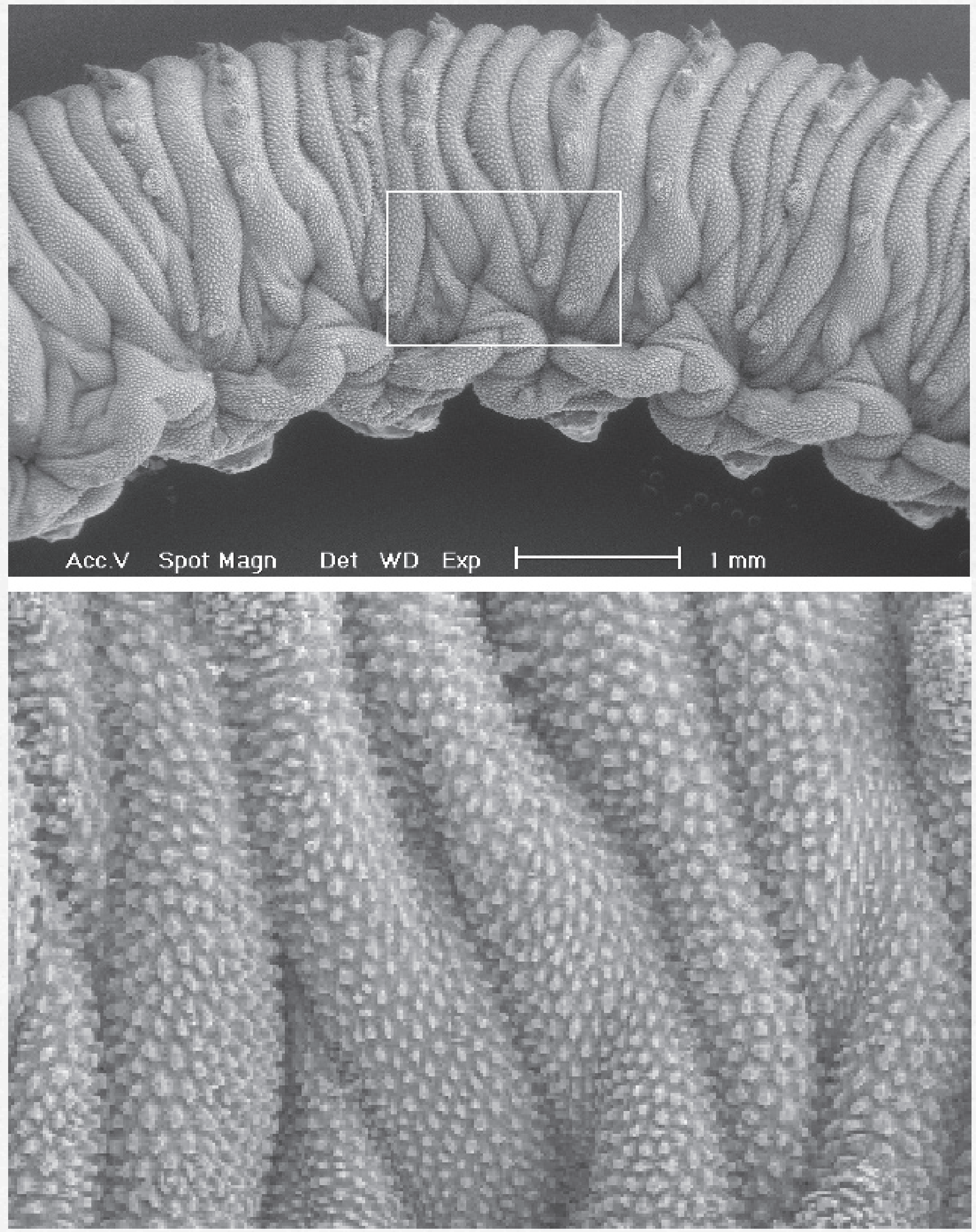

Fig. 2.2 SEM photos of a *R. micans* larva showing the cuticle surface and the microstructures which typically cover the whole body of easy bleeders. The picture above shows, in lateral view, several abdominal segments subdivided by annulets. The *inset* is magnified in the picture below

anti-wetting

Fig. 3.3 The leopard gecko *Eublepharis macularius* after water-spraying

anti-wetting

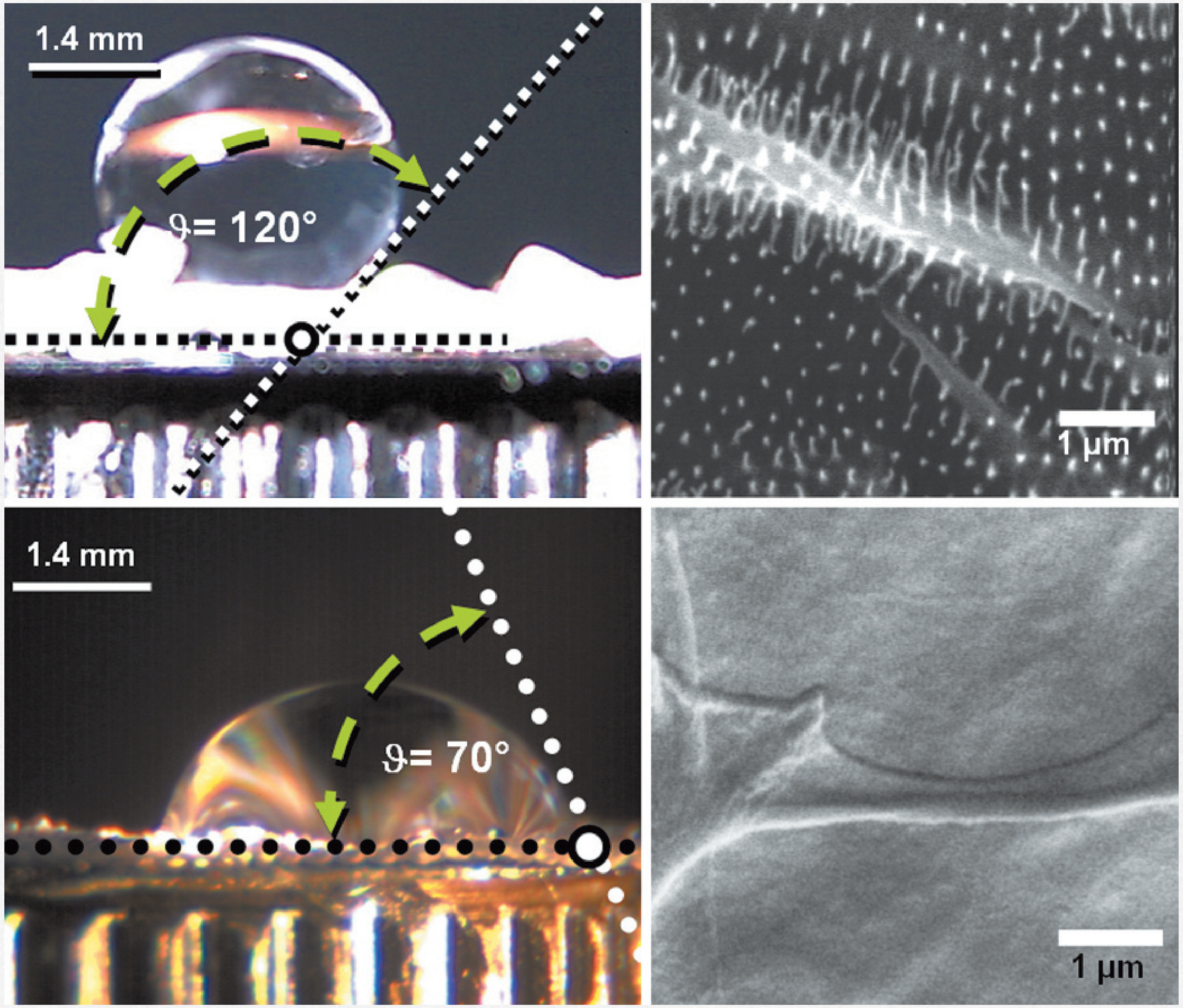

Fig. 3.2 Comparison of contact angles and surface morphology of the spinulate surface (*upper two* pictures) and the "naked" bottom side of a shed gecko skin (*lower two* pictures) (*Phelsuma laticauda*)

anti-wetting

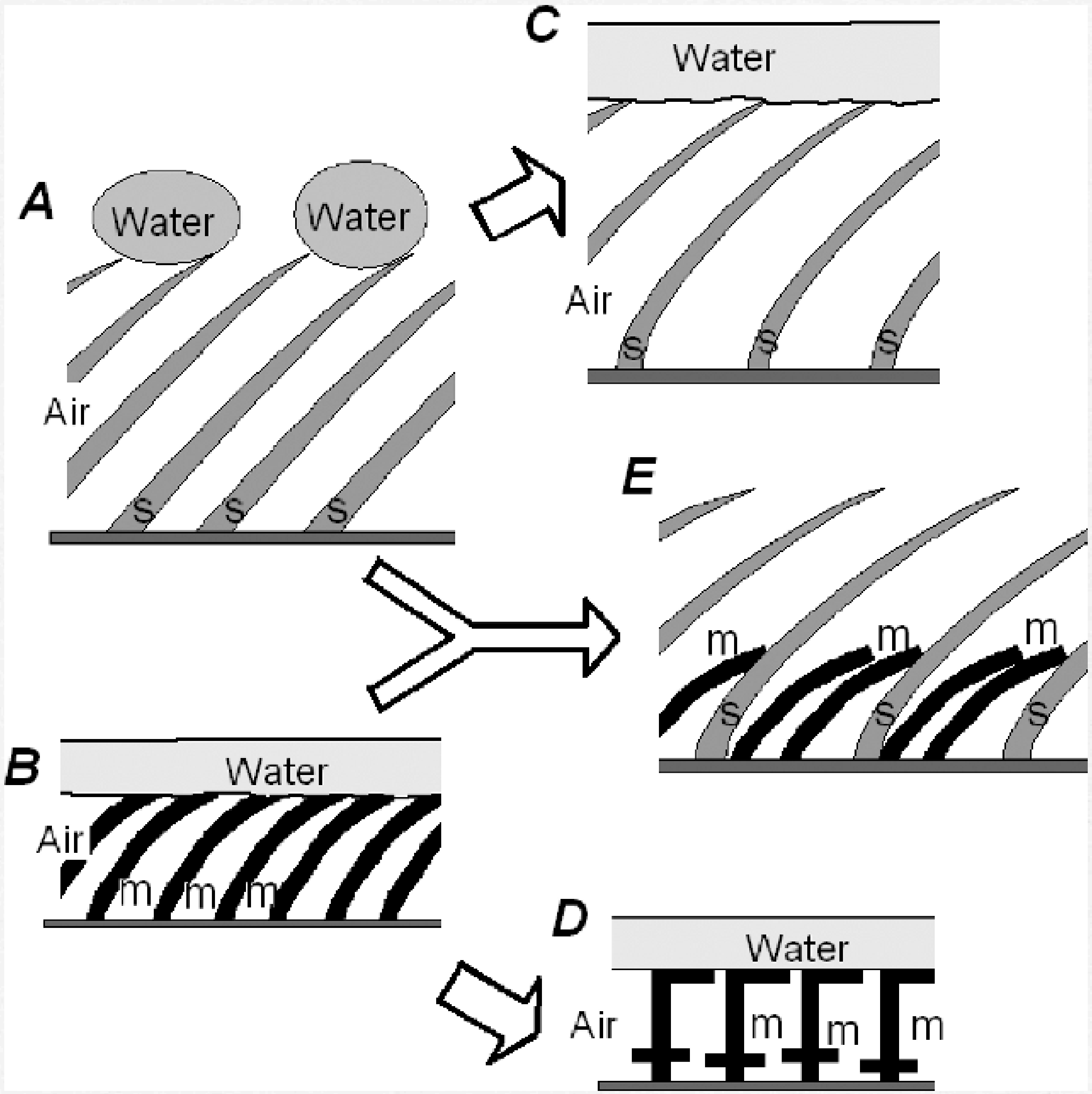

Fig. 4.6 Diagrammatic representation of anti wetting setae and/or microtrichia coverage with different functions **A**: Stiff setae, over 50–70 µm long, simple waterproofing, against irregular wetting, high aspect ratio. **B**: Common microtrichia about 7–9 µm long, compressible bubble, high aspect ratio. **C**: Setae over 50–70 µm long, compressible bubble, high aspect ratio **D**: Special microtrichia 5 µm long, with basal nodules and bent tip, true plastron, low aspect ratio. **E**: Setae with underlying microtrichia: double function cover, waterproofing and air bubble. m: microtrichia, s: setae

anti-wetting

Fig. 4.1 Thoracic cover of both setae (s) and microtrichia (m) of *Aquarius elongatum* (Gerridae)

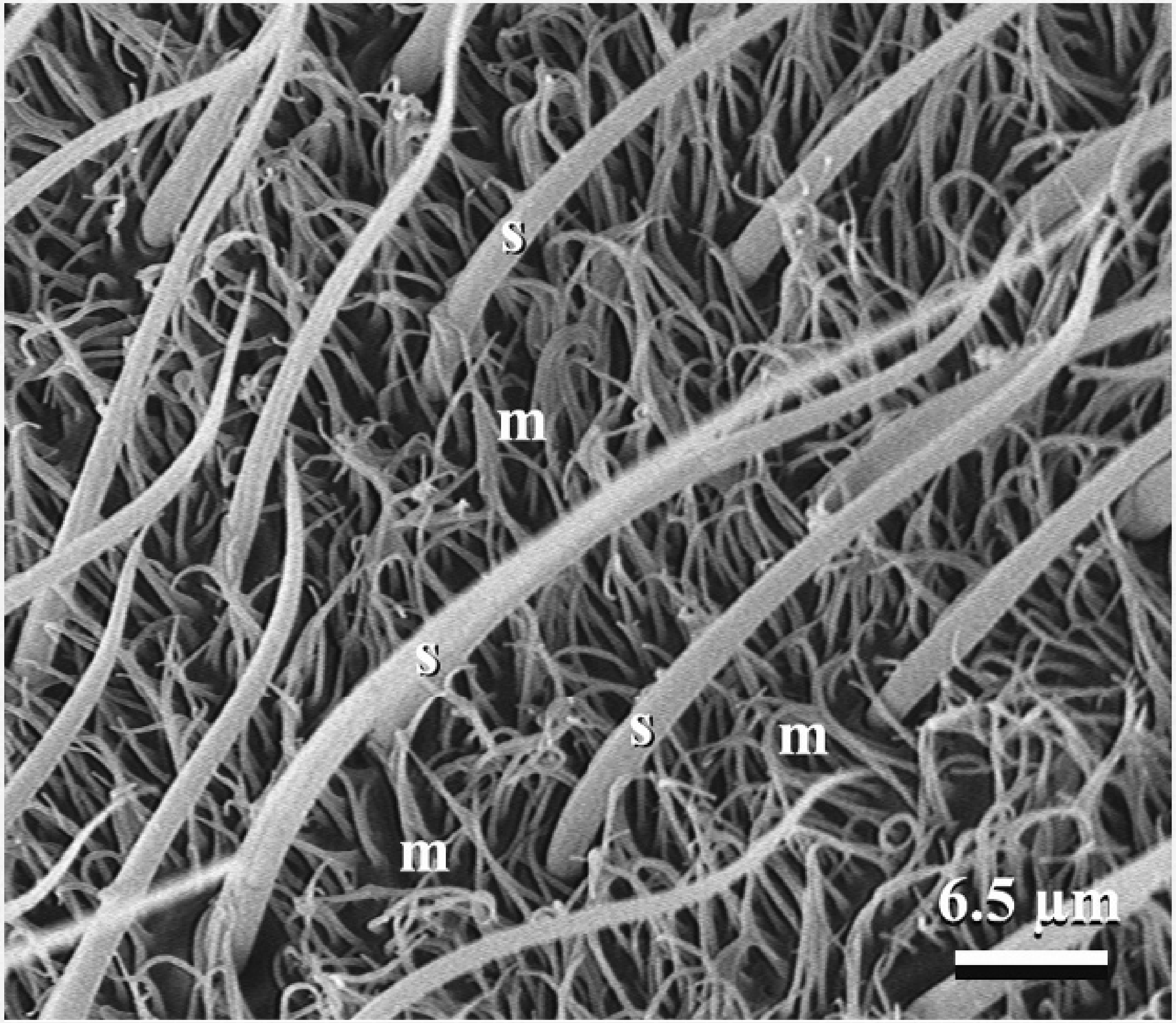

anti-wetting

Fig. 4.7 Thoracic microtrichia cover of *Halobates germanus* (Gerridae). Note "golf-club" shape heads and interlocking prolongations (*). S: setae

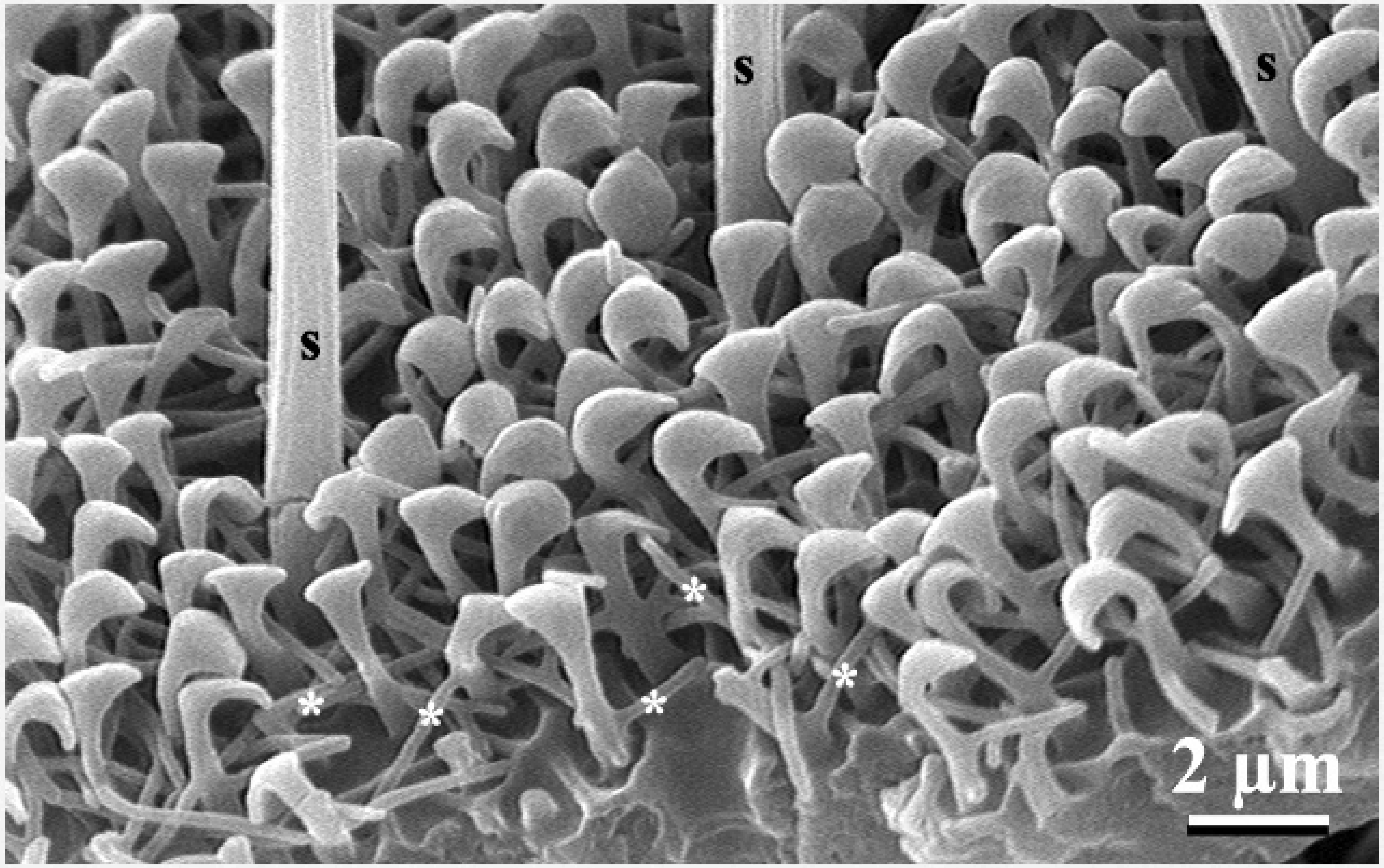

anti-wetting

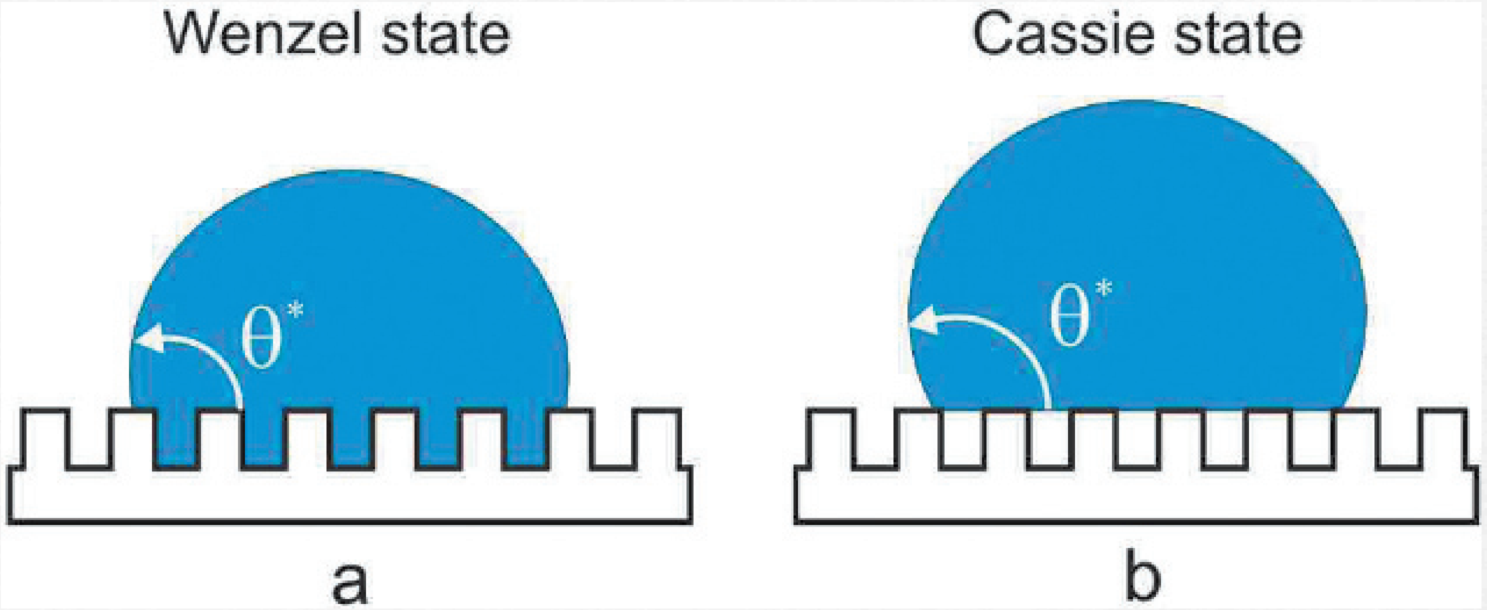

Fig. 6.2 Water droplet on a rough surface: (**a**) sunk into the structure (Wenzel state) (**b**) resting on top of the structure like a fakir on a bed of nails (Cassie state) θ^* – real measured contact angle

anti-wetting

Fig. 6.3 Water droplet on *Salvinia oblongifolia* leaf. The silvery shine is caused by air trapped between trichomes, resulting in a total reflection of the drop's lower surface

anti-wetting

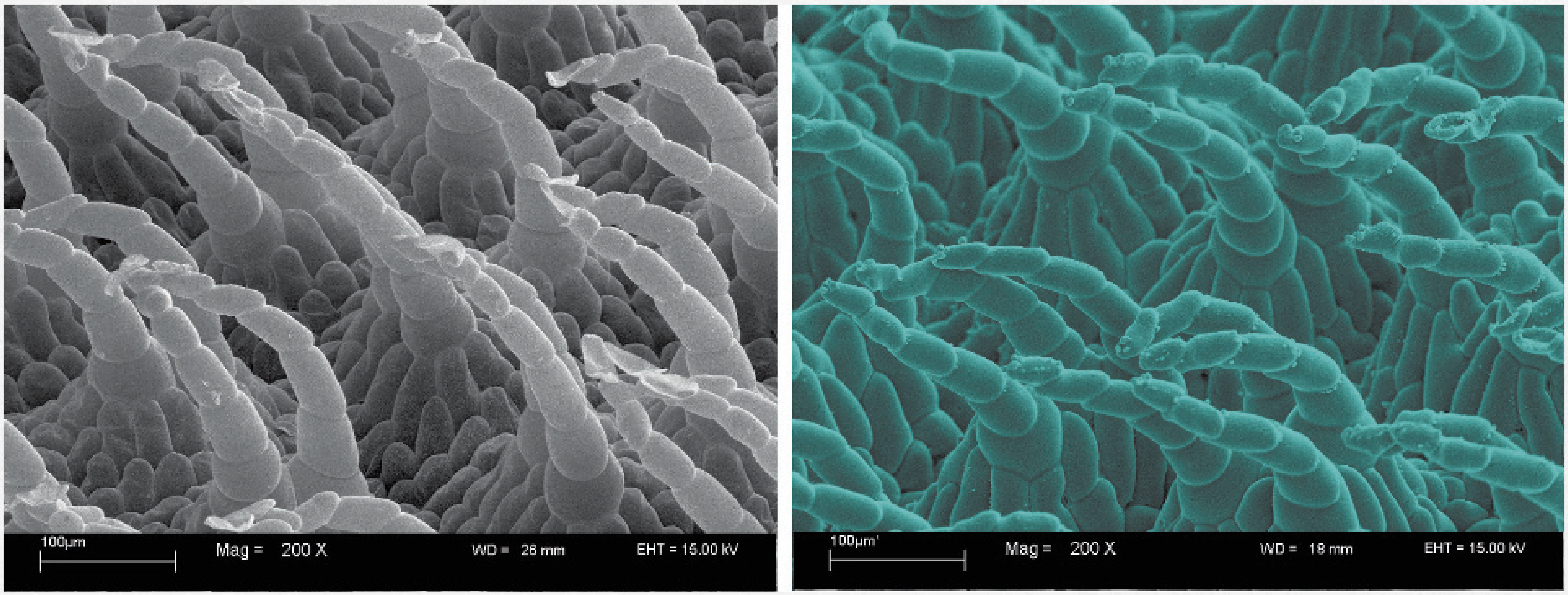

Fig. 6.4 Comparison of *Salvinia oblongifolia* trichomes (SEM; magnification 200×) *left*: plant surface; *right*: artificial microreplica

anti-wetting

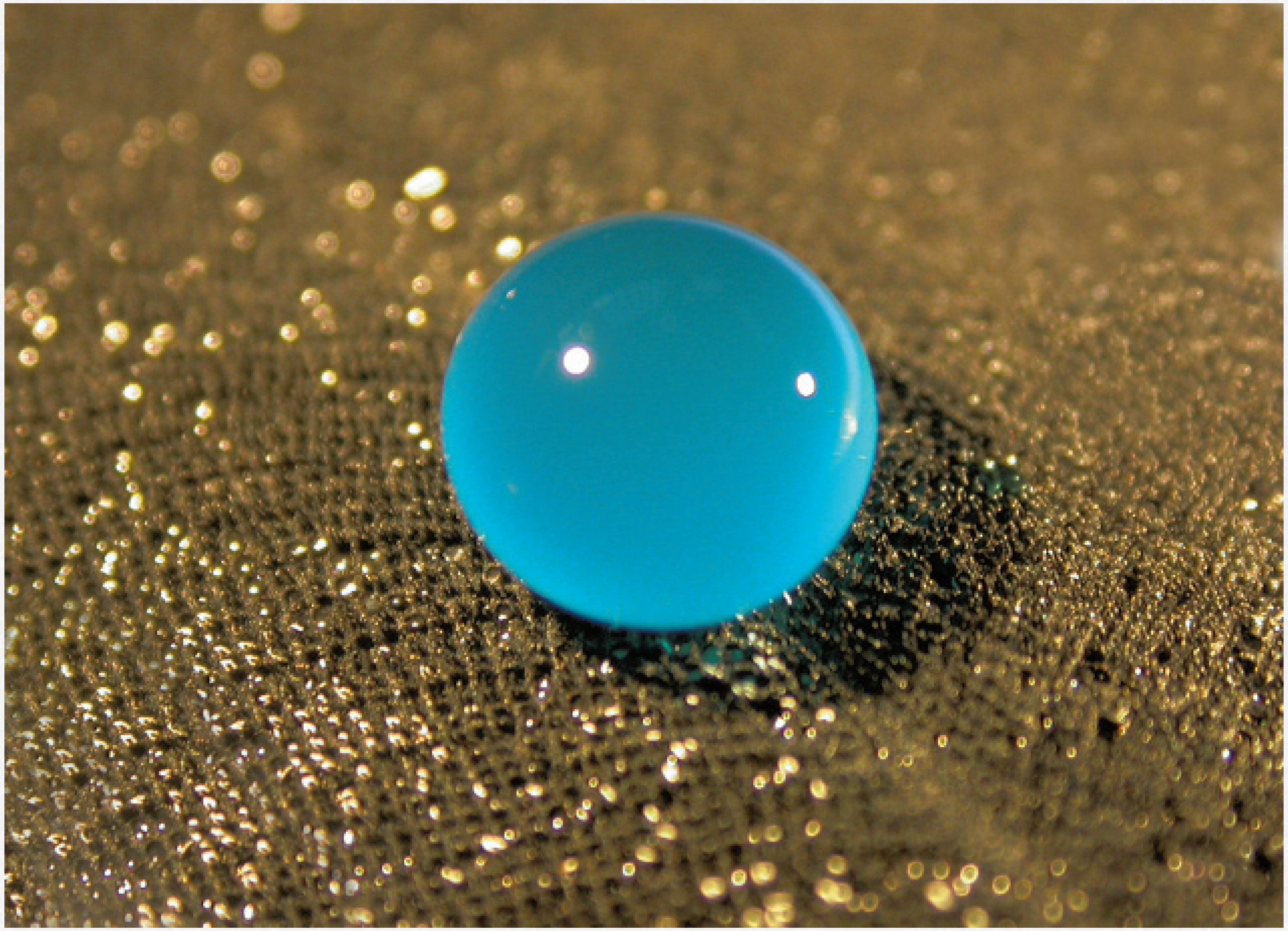

Fig. 6.5 Water droplets (stained with food dye) form a nearly perfect sphere on the acrylic replica of *Salvinia oblongifolia*

transport

Fig. 8.8 Aerial root of *Epidendrum speciosus*. V: Velamen radicum. E: Exodermis. C: Cortex. S: Stele. Scale bar: 100 μm

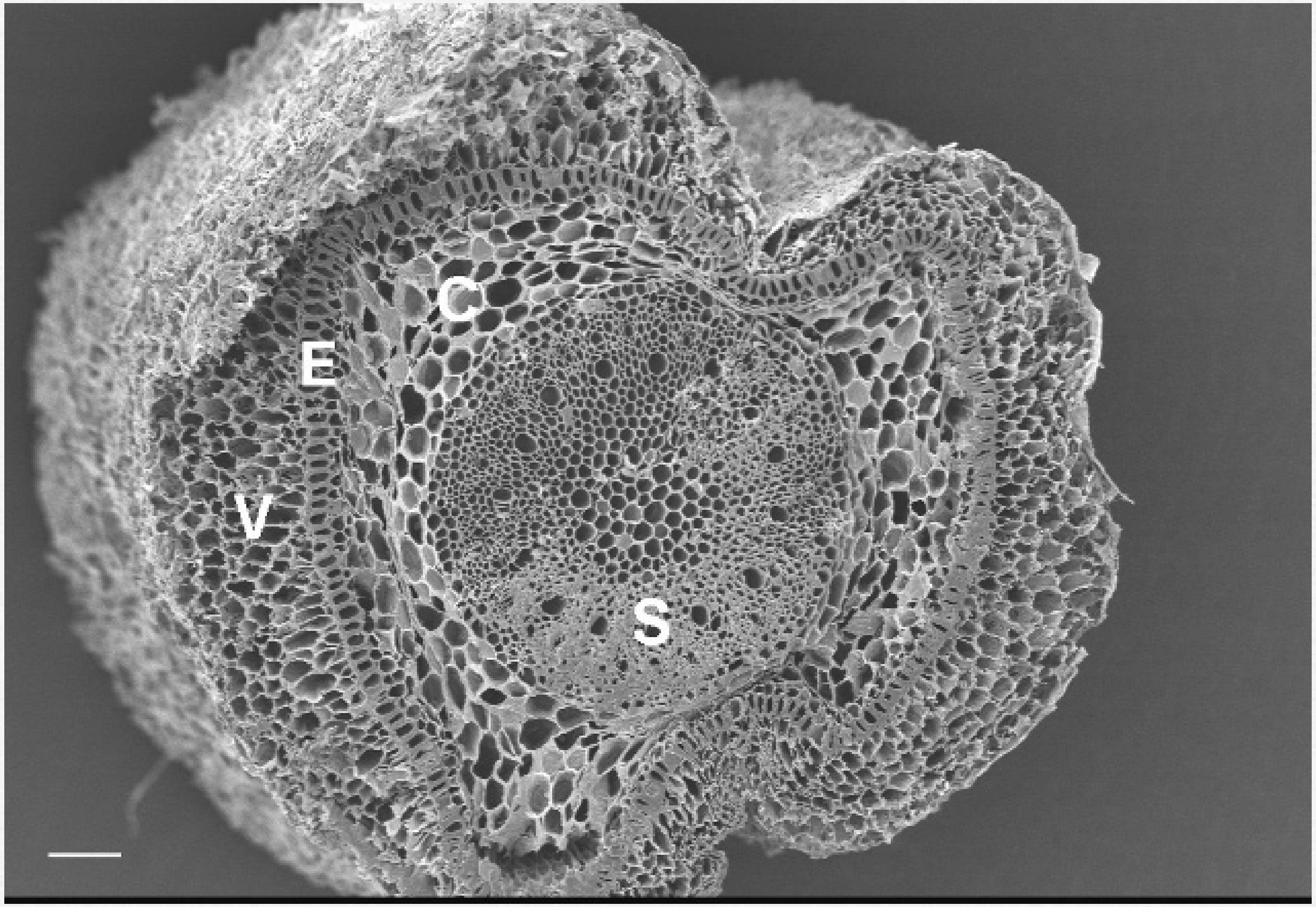

desert beetle: water transport

desert beetle: water transport

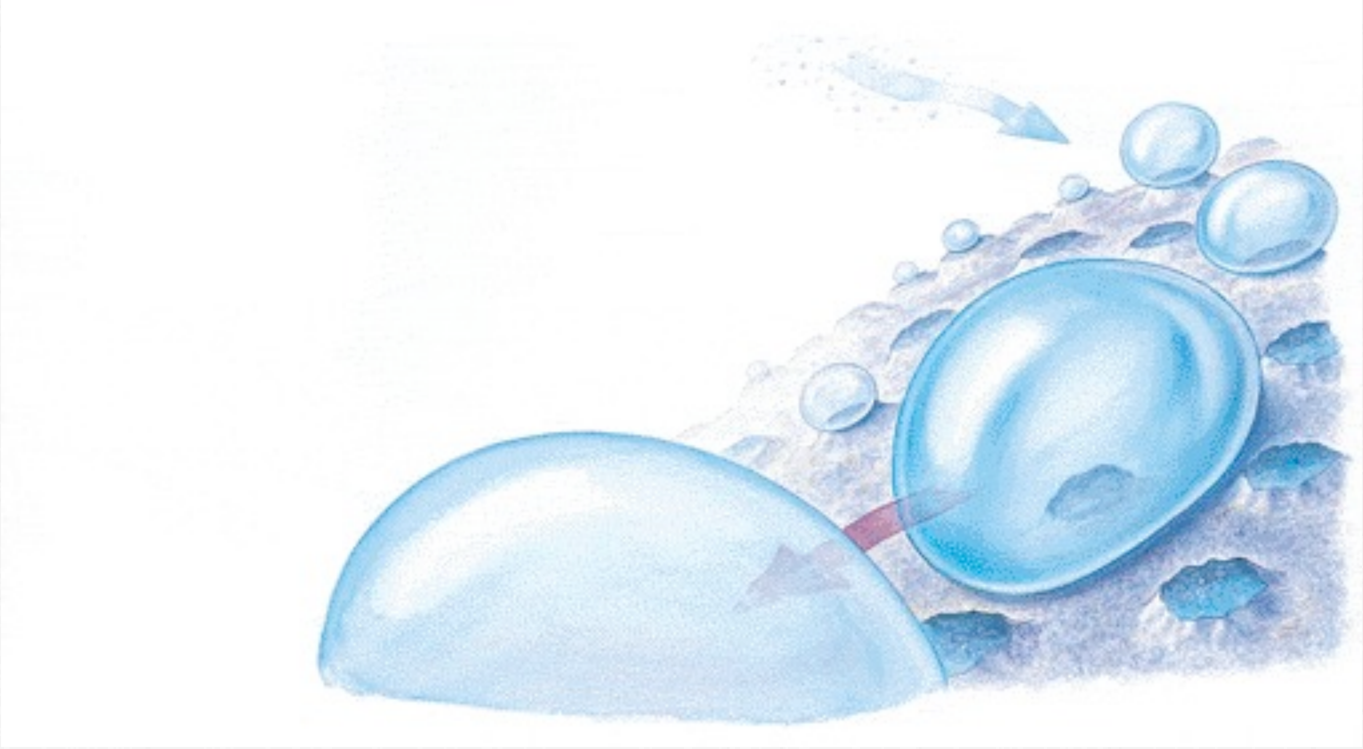

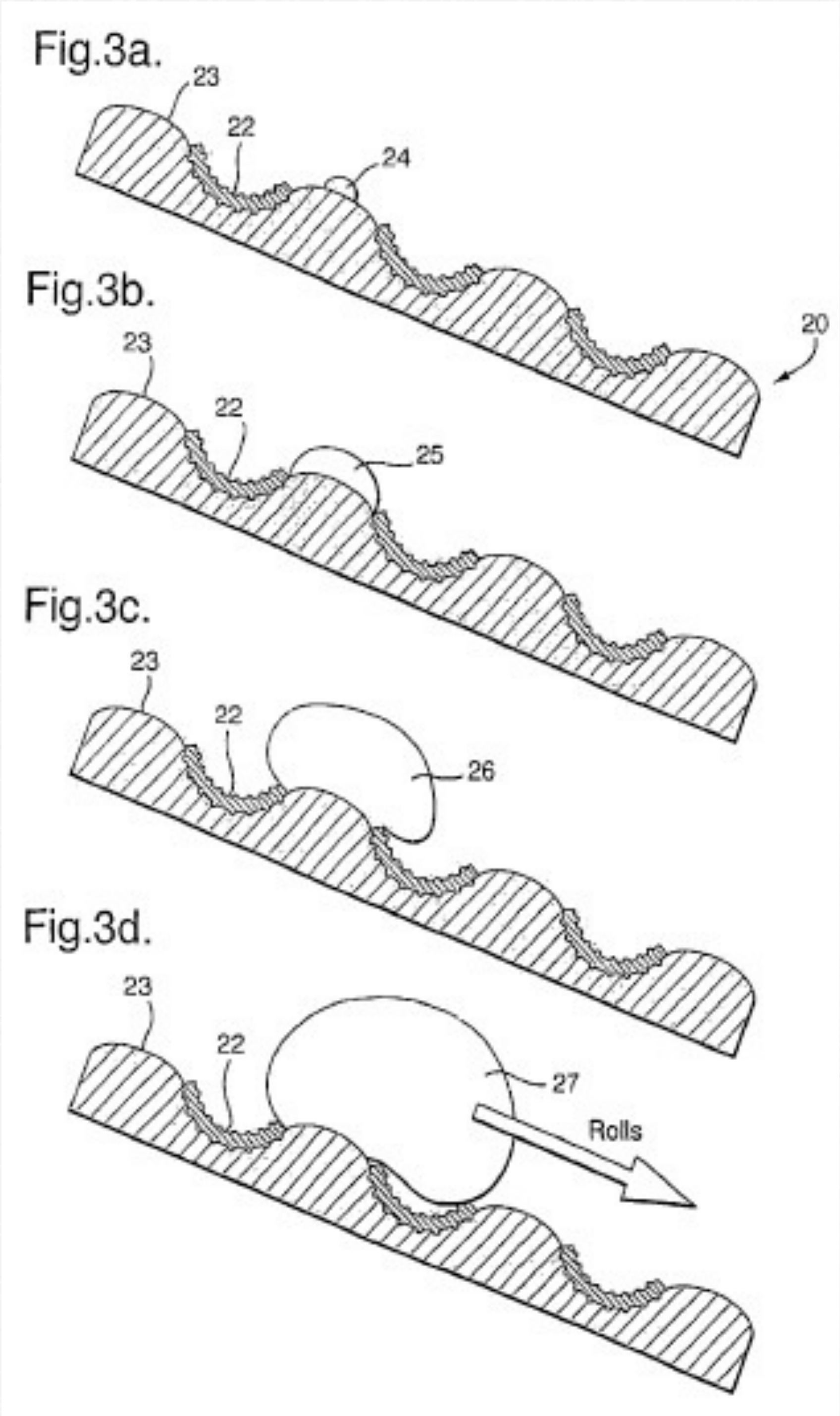

desert beetle: water transport

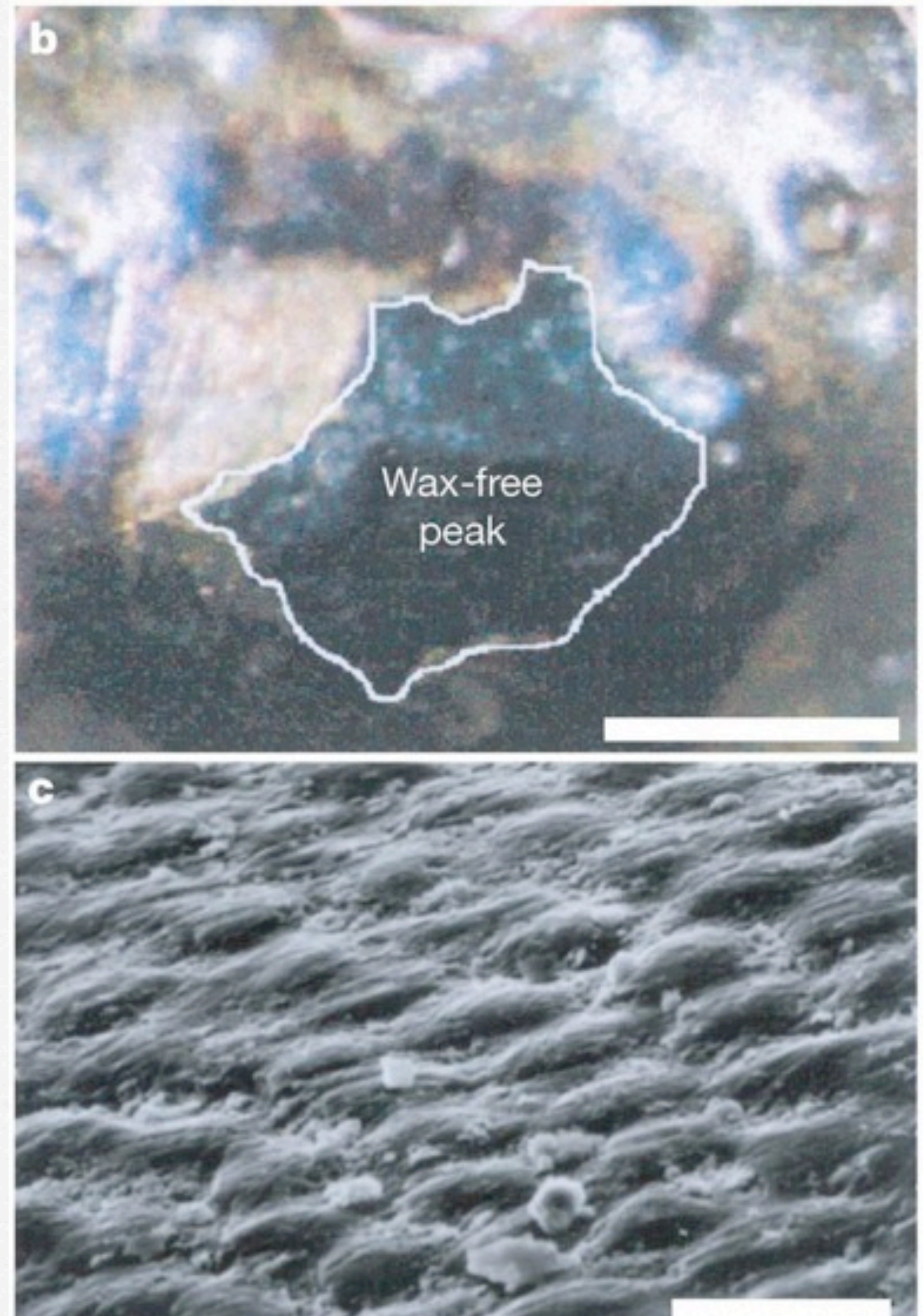

sensor hairs

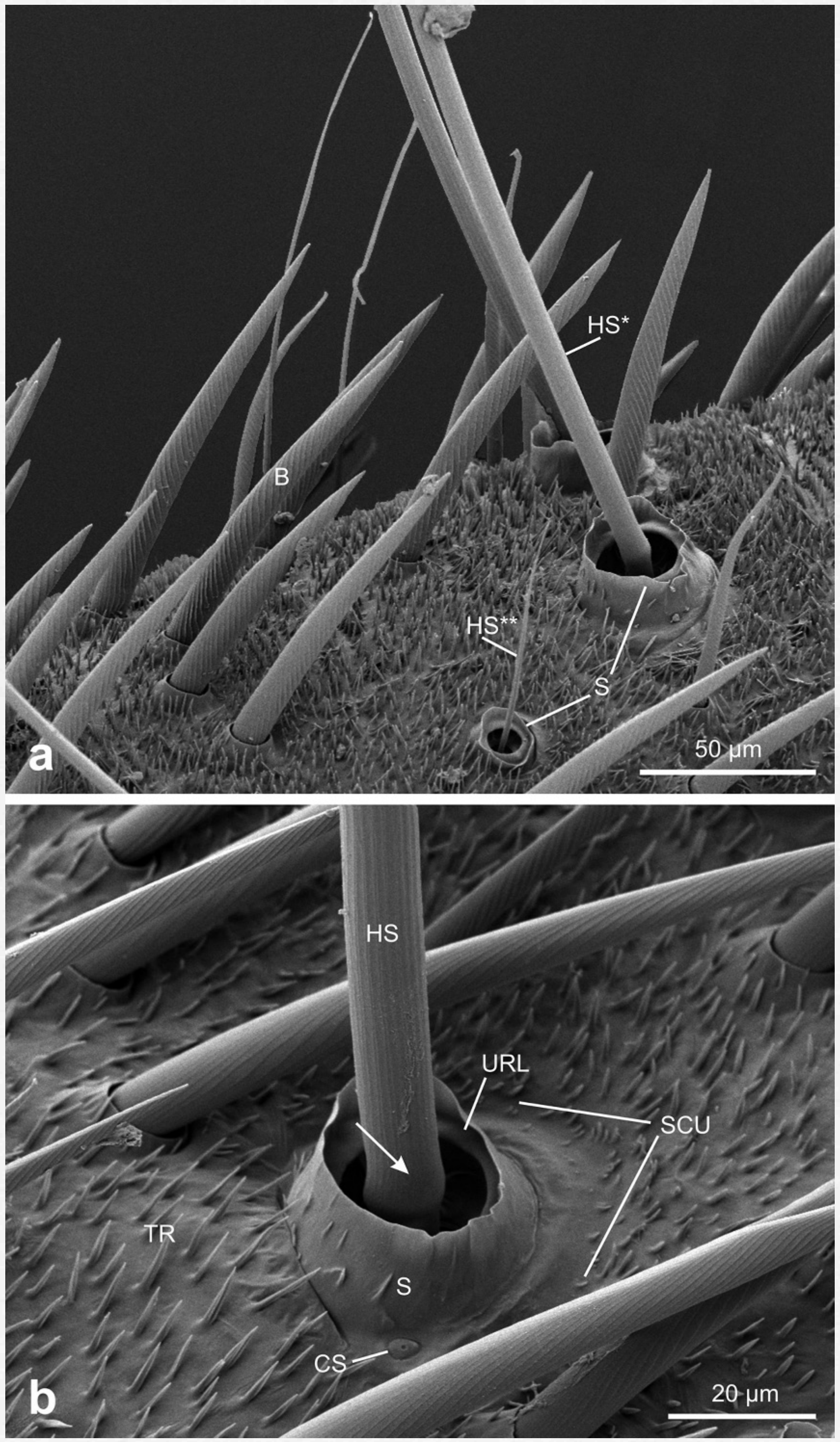

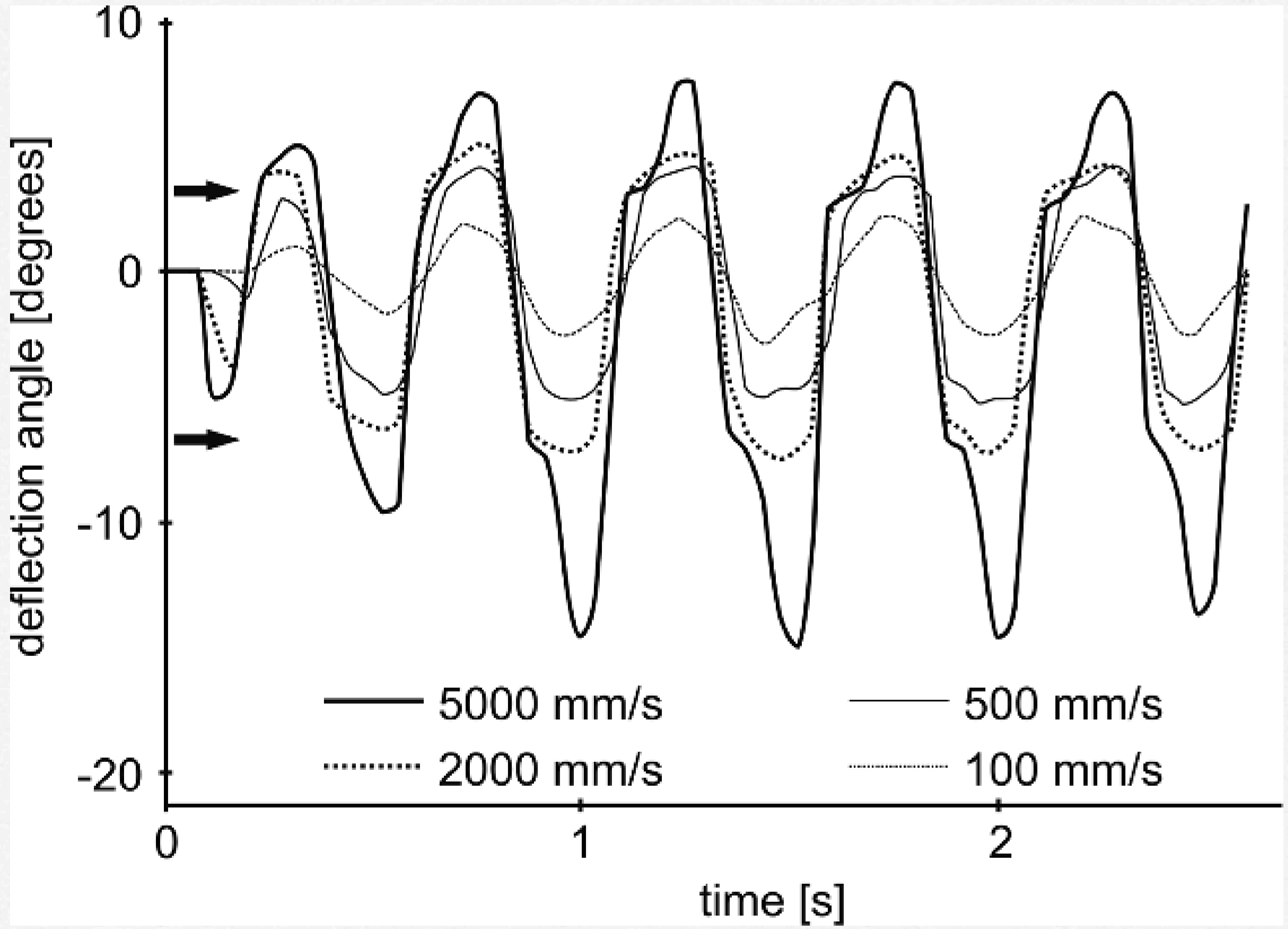

optics

optics

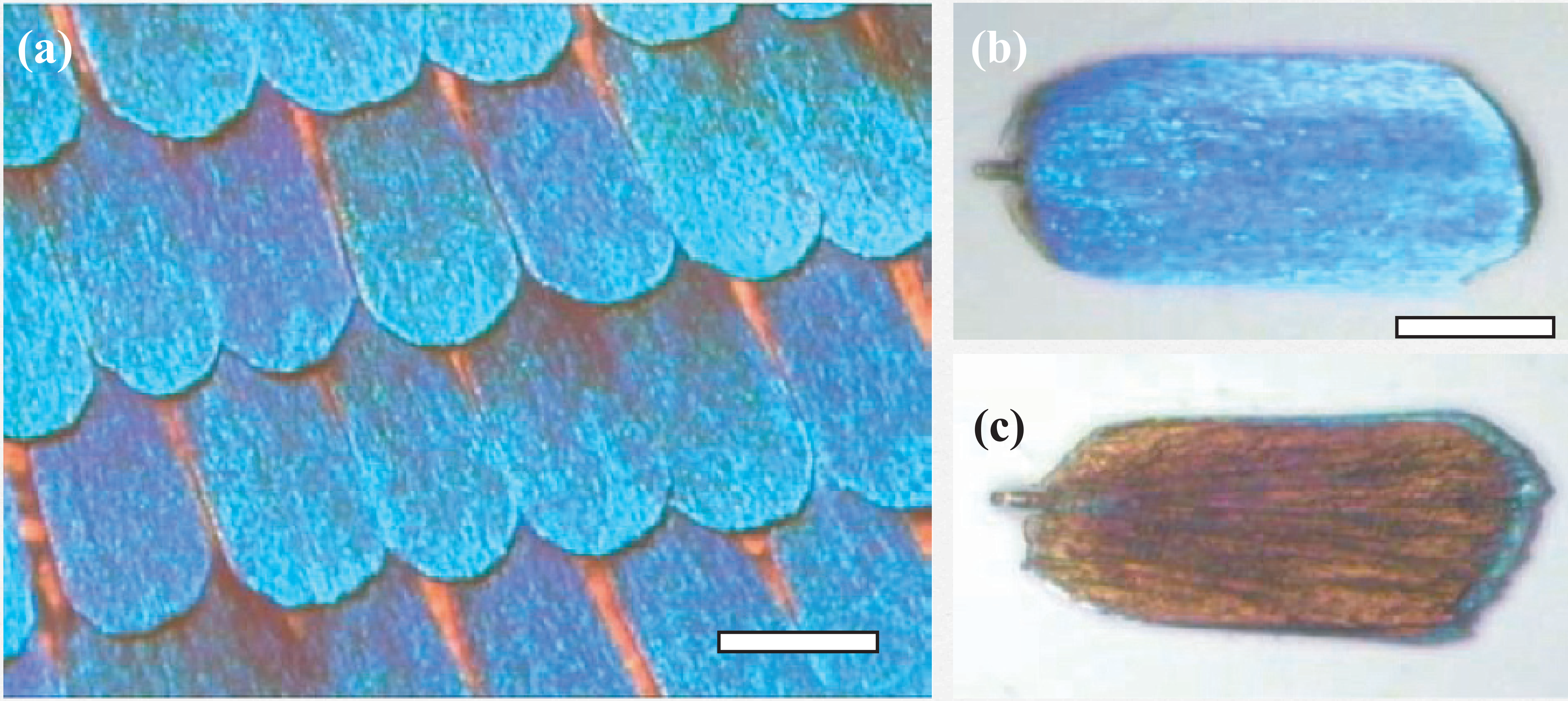

Fig. 12.1 **(a)** optical image of wing-scales on *M. rhetenor*, showing the scales as the seat of the colour; **(b)** dorsal and **(c)** ventral surface of a single iridescent *M. rhetenor* scale [Scale bars: (a) 100 μm; (b) and (c) 25 μm]

optics

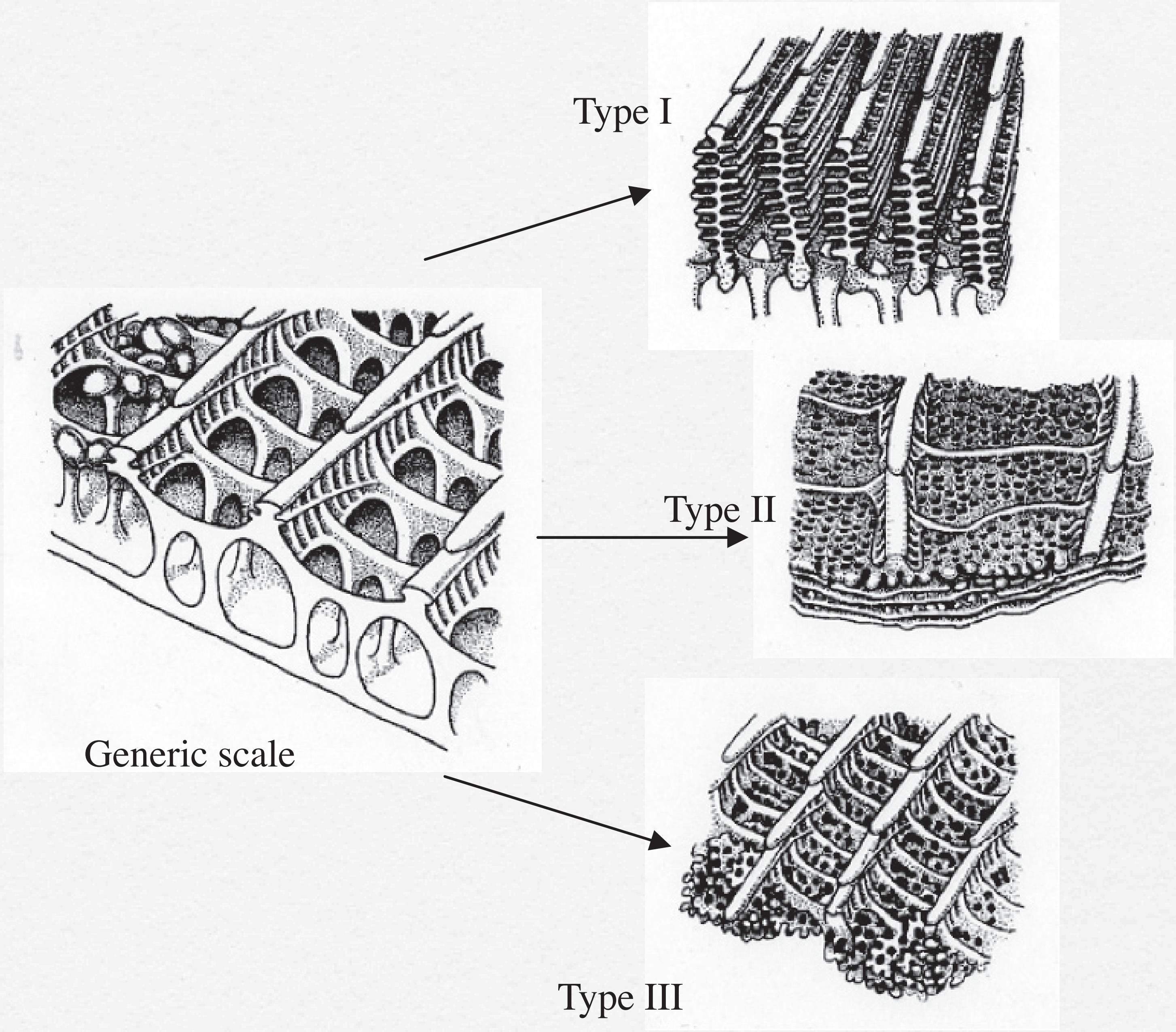

Fig. 12.2 Schematic diagram to show the classification of the microstructure of iridescent butterfly scales. (Schematic diagrams reprinted with permission from H. Ghiradella and Wiley-Liss, © 1998.)

optics

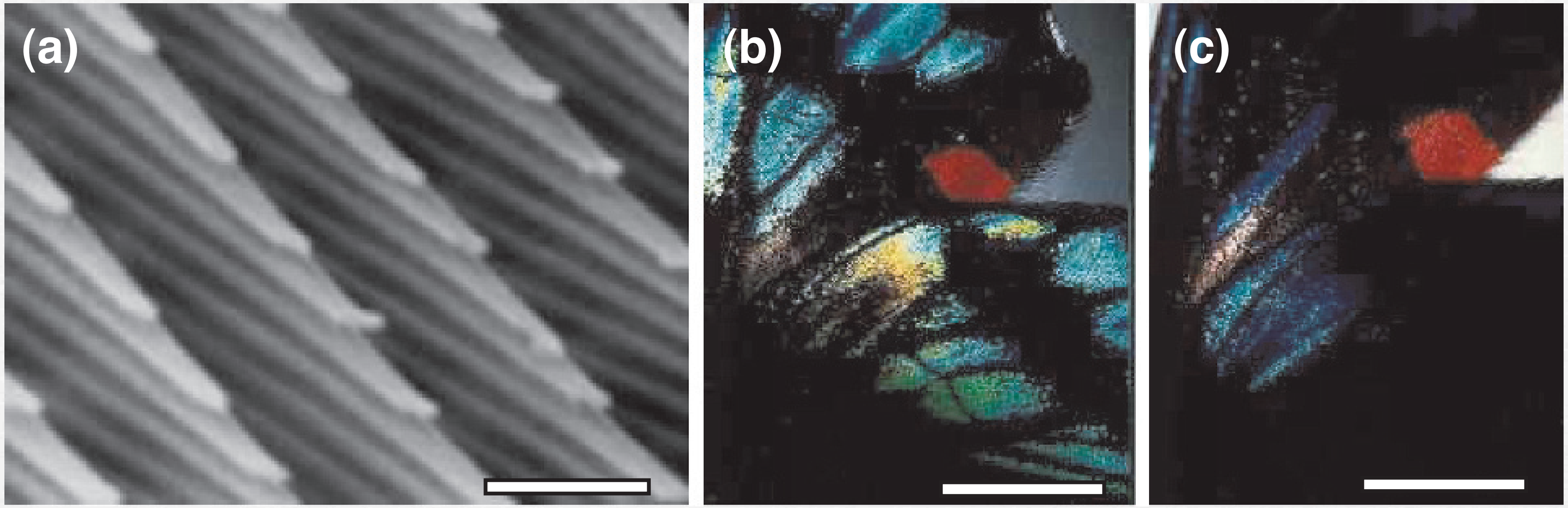

Fig. 12.3 **(a)** SEM micrograph showing type Ib scale microstructure of the butterfly *A. meliboeus*. The multilayering within the ridging is clearly tilted; **(b)** and **(c)** optical real-colour photographs of the same region of *A. meliboeus* wing under identical diffuse illumination, but with a 10 degree wing tilt between them. [Scale bars: (a) 700 nm, (b) and (c) 5 mm]. (Reprinted with permission from *Nature* (**410,** 36) © 2001). Macmillan Magazines Ltd.

optics

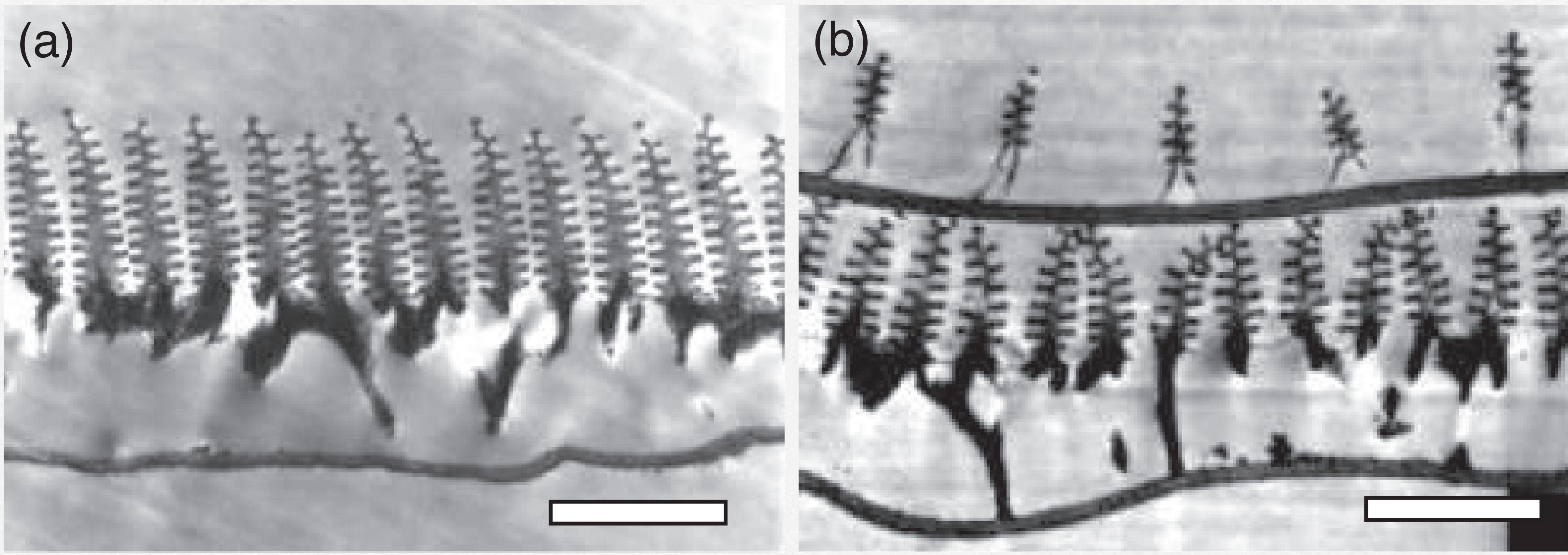

Fig. 12.5 TEM images of cross-sections through iridescent scales of **(a)** *M. rhetenor* and **(b)** *M. didius*. [Scale bars; 1.5 μm]

optics

(a) (b)

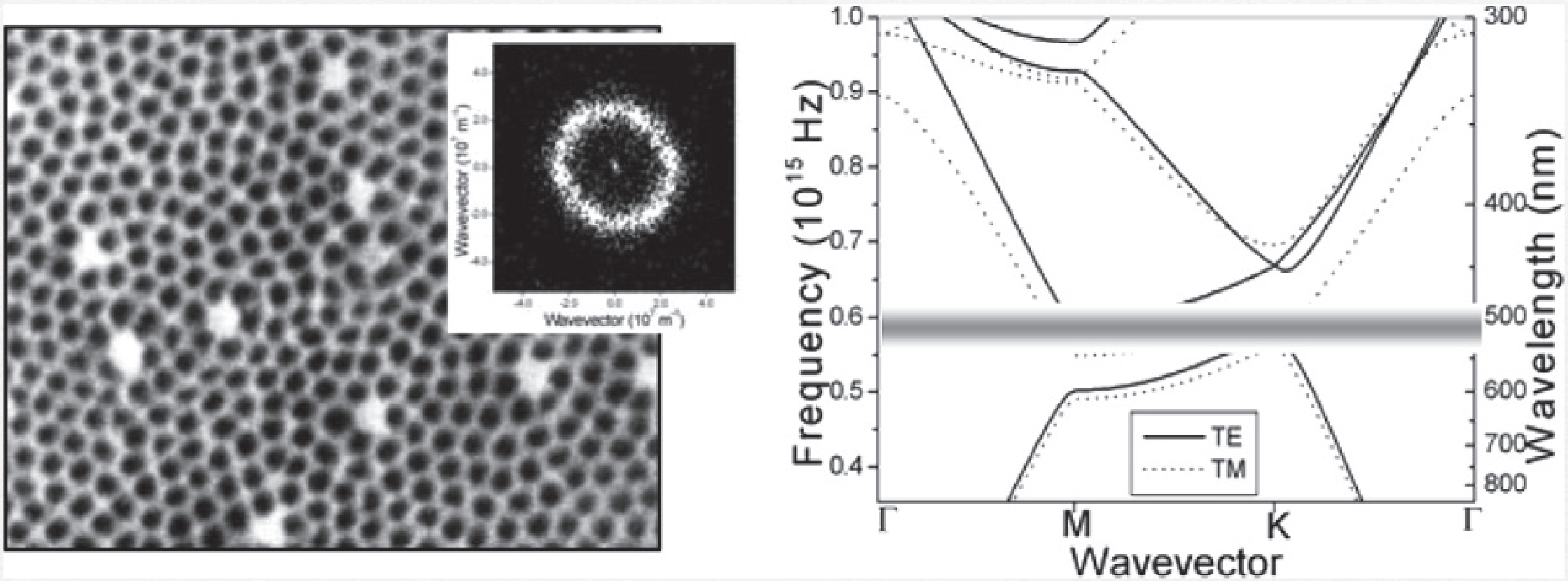

Fig. 12.17 **(a)** SEM image of the underside of the PCS in a *P. nireus* coloured scale showing quasiperiodicity (inset: 2D-fast Fourier transform of the image in a). **(b)** Band diagram of *P. nireus* intra-domain PCS structure (horizontal bar centred at 505 nm represents fluorescence emission FWHM)

optics

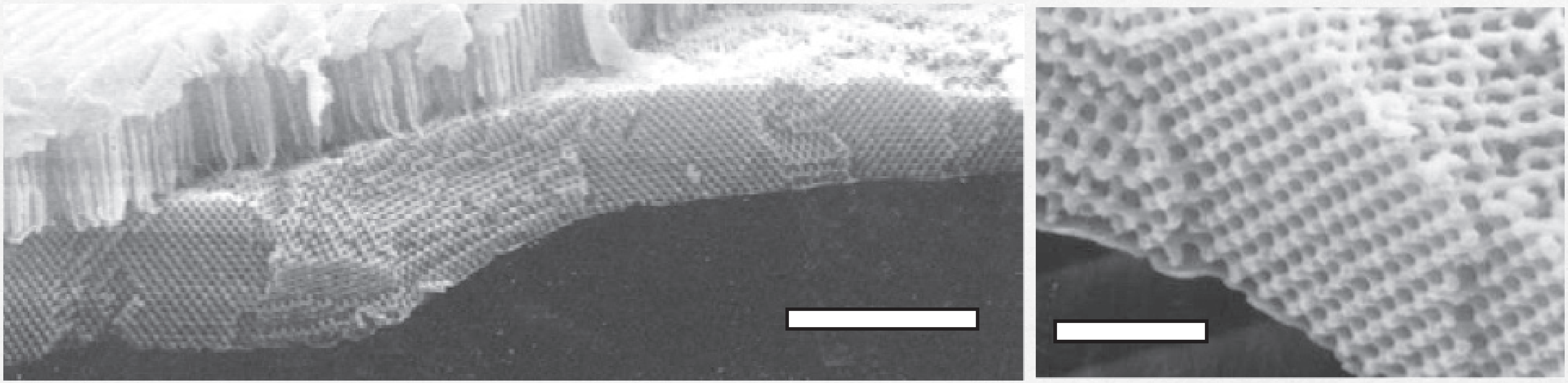

Fig. 12.12 SEM images of the sectioned side of an iridescent scale from *P. sesostris* showing its regular lattice of cuticle sited below a dense array of ridging. [Scale bar: 5 μm (*left*) and 1 μm (*right*)]. Reprinted with permission from *Nature* (**424**, 852–856) © 2003). Macmillan Magazines Ltd

optics

Fig. 12.13 Optical micrographs; **(a)** *P. sesostris* scales under normal illumination, and **(b)** a single *P. sesostris* scale viewed in reflection under illumination with linearly polarized white light while the image was captured through a crossed linear analyser. [Scale bar: (a) 50 µm and (b) 20 µm]

optics

Fig. 13.16 The opal structure. (**A**) A 110 Ma opalized bivalve (Mollusca) shell from Australia. (**B**, **C**) The weevil *Metapocyrtus* sp. (**B**) Scanning electron micrograph of the opal analogue positioned within a single scale; white scale bar = 1 μm. (**C**) Whole animal; the opal structure lies within the turquoise scales

A

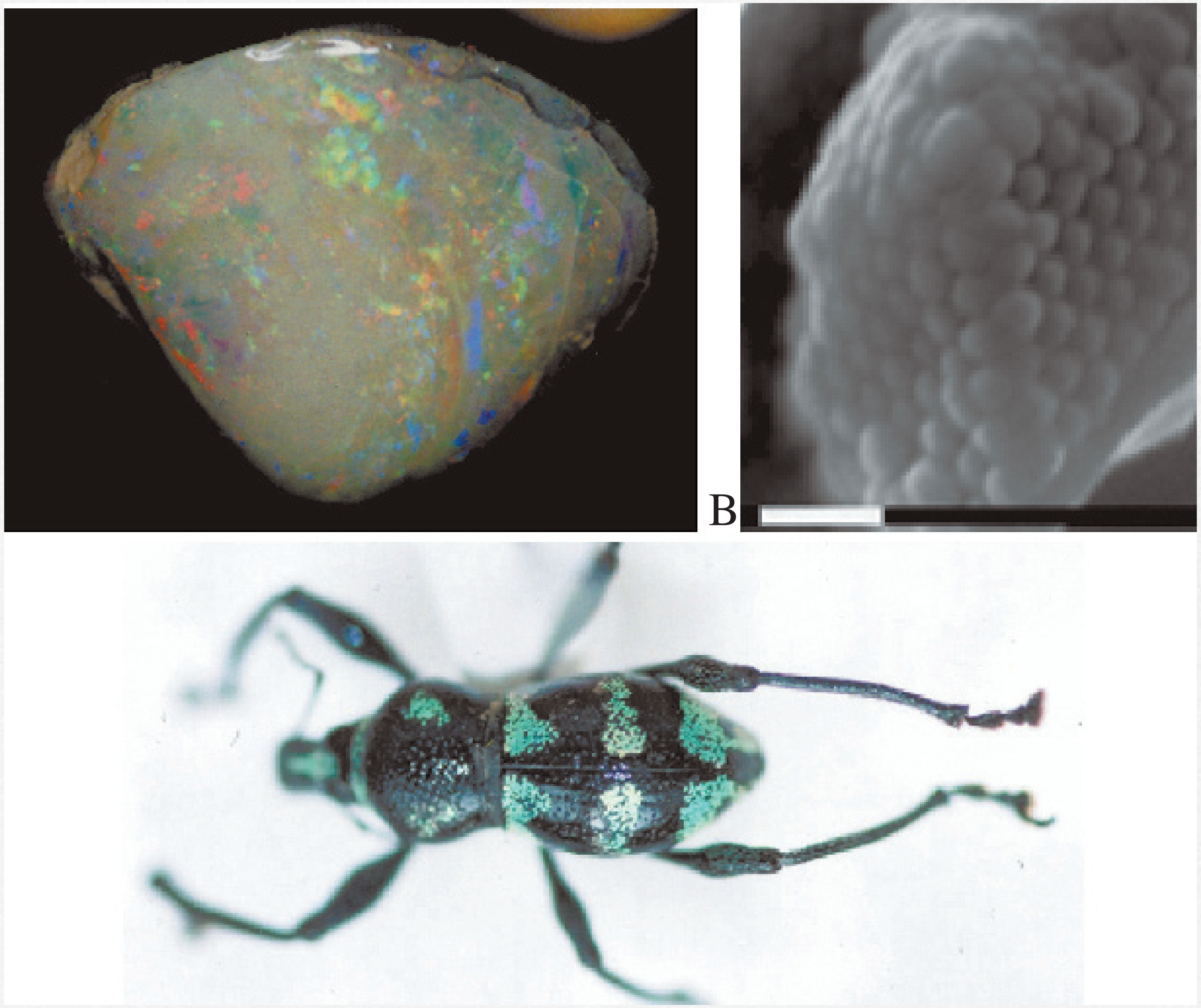

B

C

optics

Fig. 13.17 The “inverse opal” structure. (**A**) Three-dimensional reconstruction of the inverse opal in the wing scale of the butterfly *Teinopalus imperialus* (periodicity = 250 nm). (**B**, **C**) *Eupholus nickerli*. (**B**) Whole animal. (**C**) Transmission electron micrograph of a transverse section through the scale of a foot, showing the inverse opal structure arranged in domains (this is how the inverse opal structure appears in a single section); scale bar = 1 μm

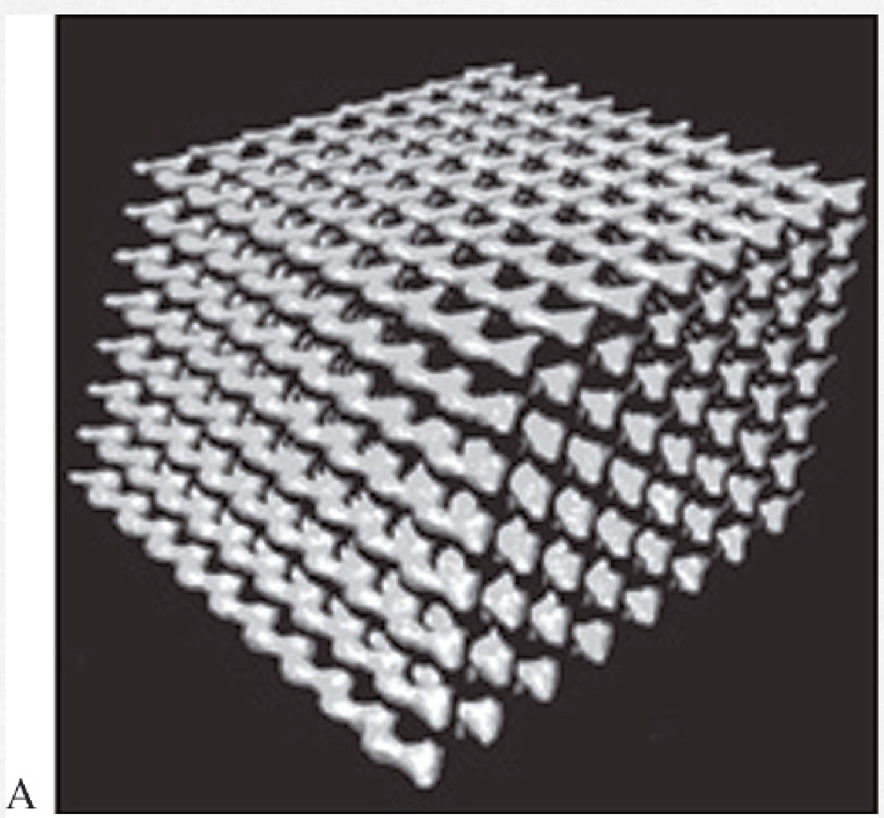

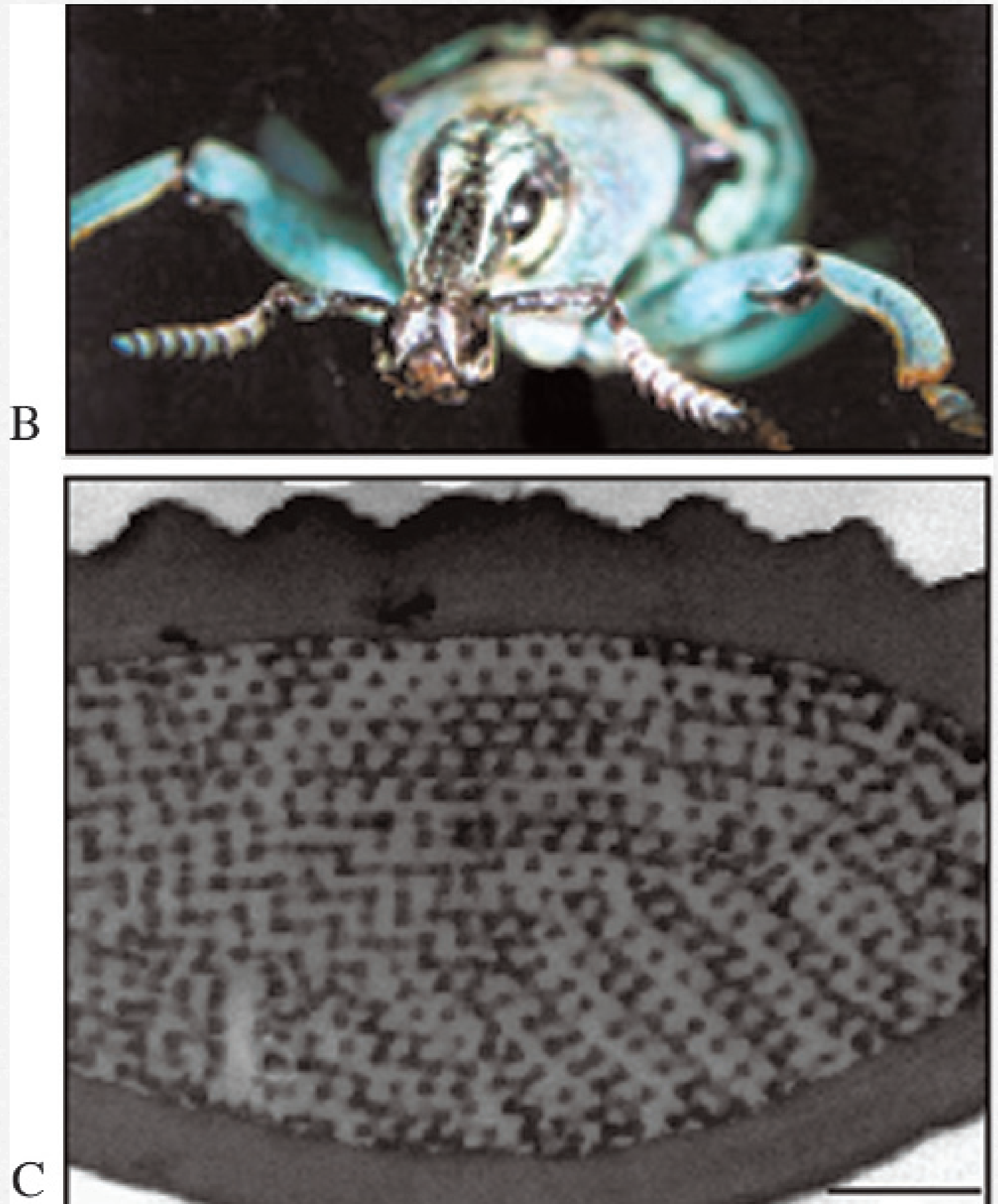

optics

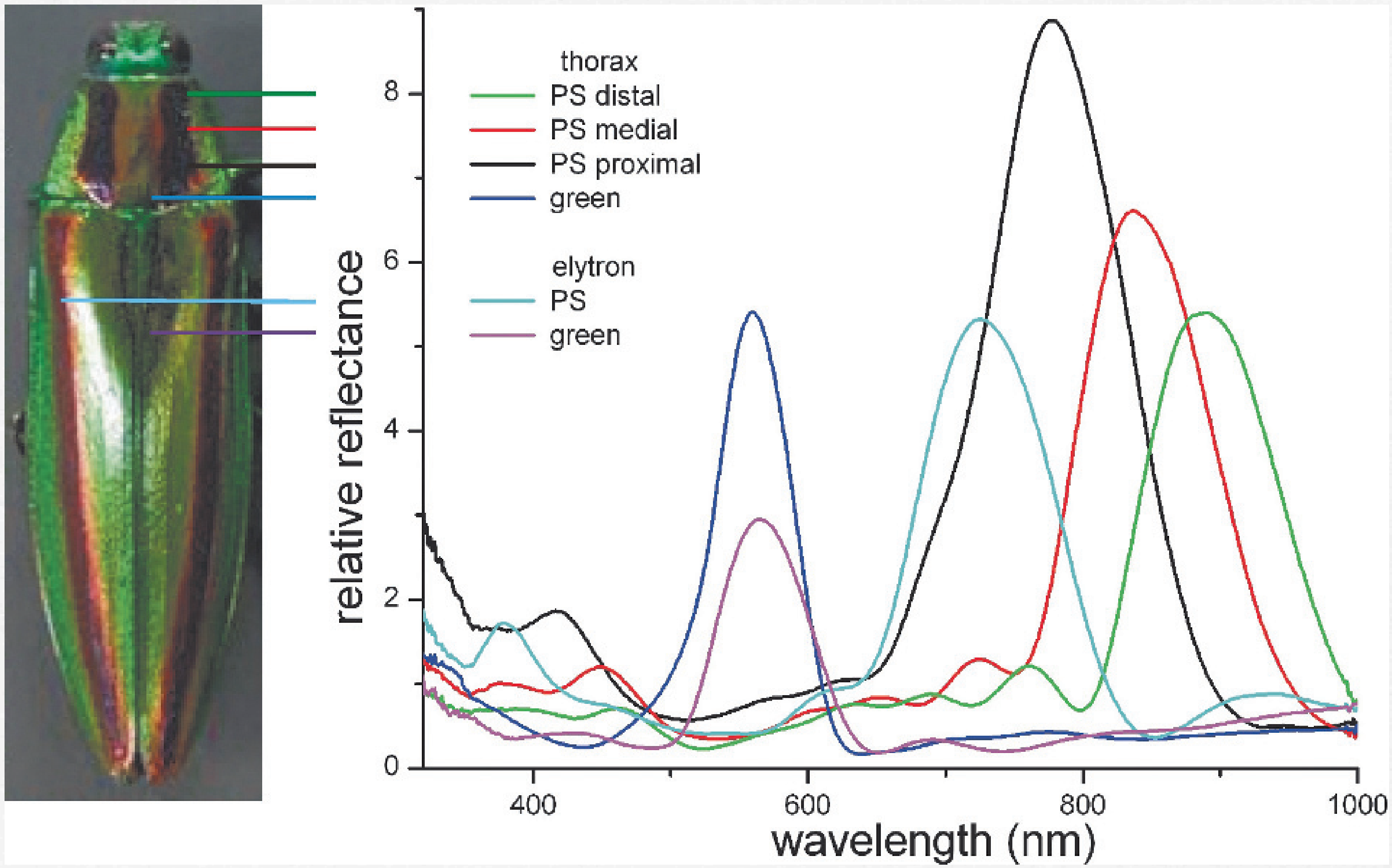

Fig. 14.1 The jewel beetle, *Chrysochroa fulguidissima* (size about 35 mm × 14 mm), and reflectance spectra measured with a fiber optic spectrometer relative to a white diffusing standard. The thorax and elytra of the jewel beetle are iridescent green, interrupted by purplish lanes (PL). The reflectance spectra of the green areas peak in the green wavelength range at about 550 nm, as expected. The reflectance of the purple lanes of the elytra, however, peak in the deep-red above 700 nm, and the stripes at the thorax reflect locally maximally at about 900 nm. The reflectance is low at green wavelengths, and the purplish impression is due to the tail of the reflectance peak in the red and a slightly higher reflectance in the blue

adhesion enhancement

adhesion enhancement

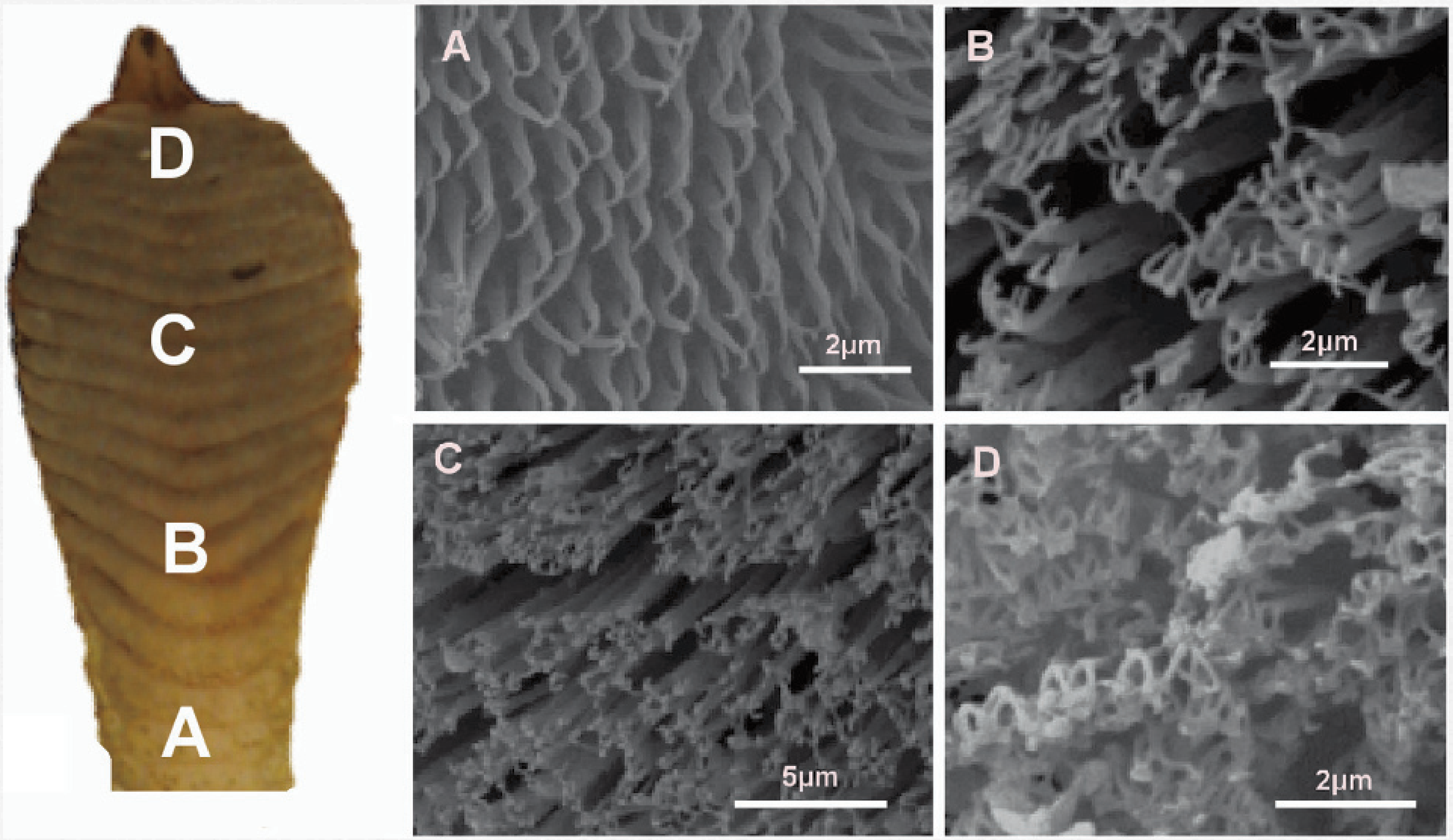

Fig. 5.2 Variation in setal size and complexity from the proximal (A) to the distal end of the digit (D) of the Tokay gecko (*Gekko gecko*). **A** curved spines carried on the basal scales of the digit **B** branched prongs carried on proximal lamellae **C** setae carried on proximally located scansors **D** setae carried on the distalmost scansors

adhesion enhancement

gecko setae

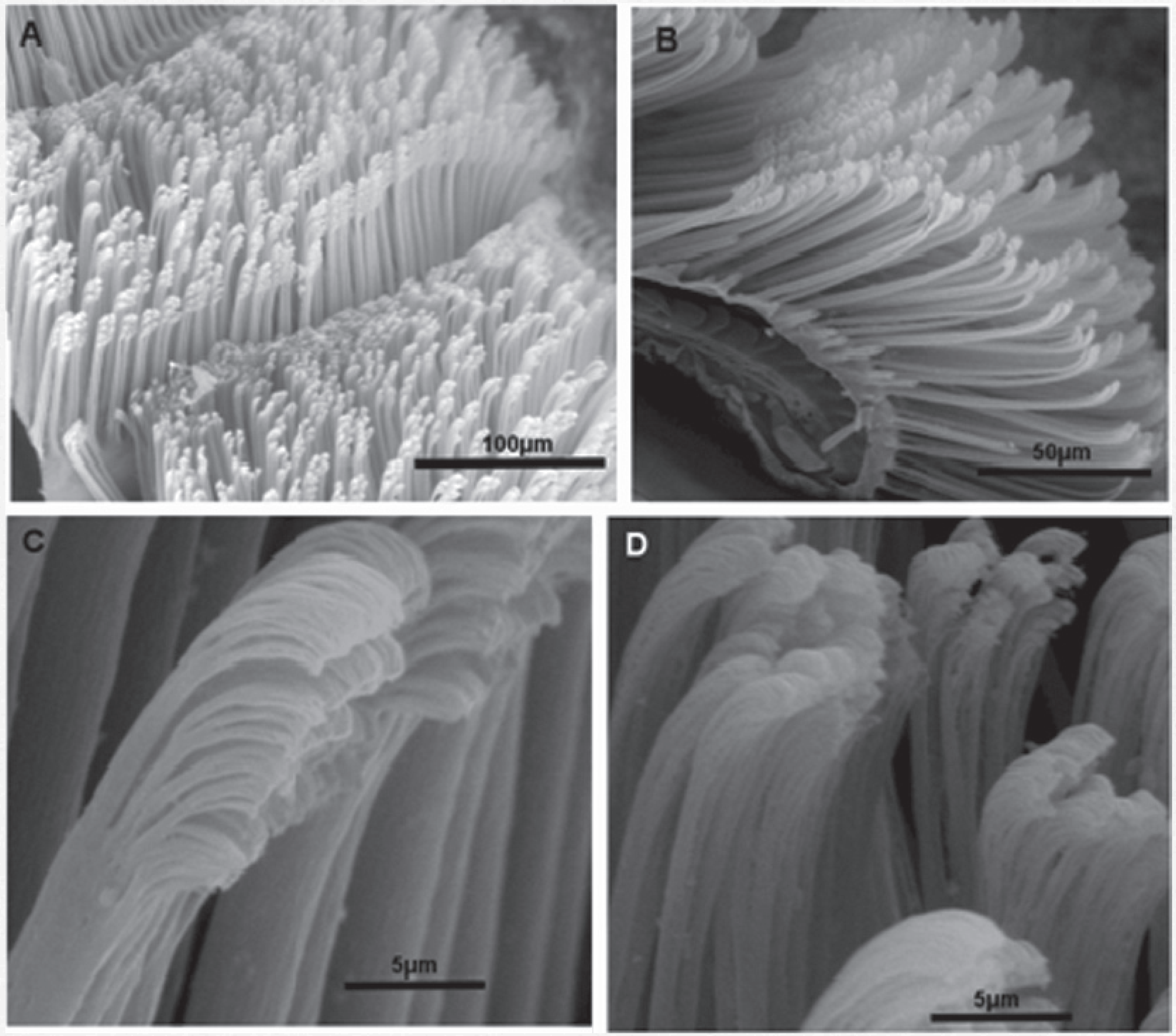

adhesion enhancement

adhesion enhancement

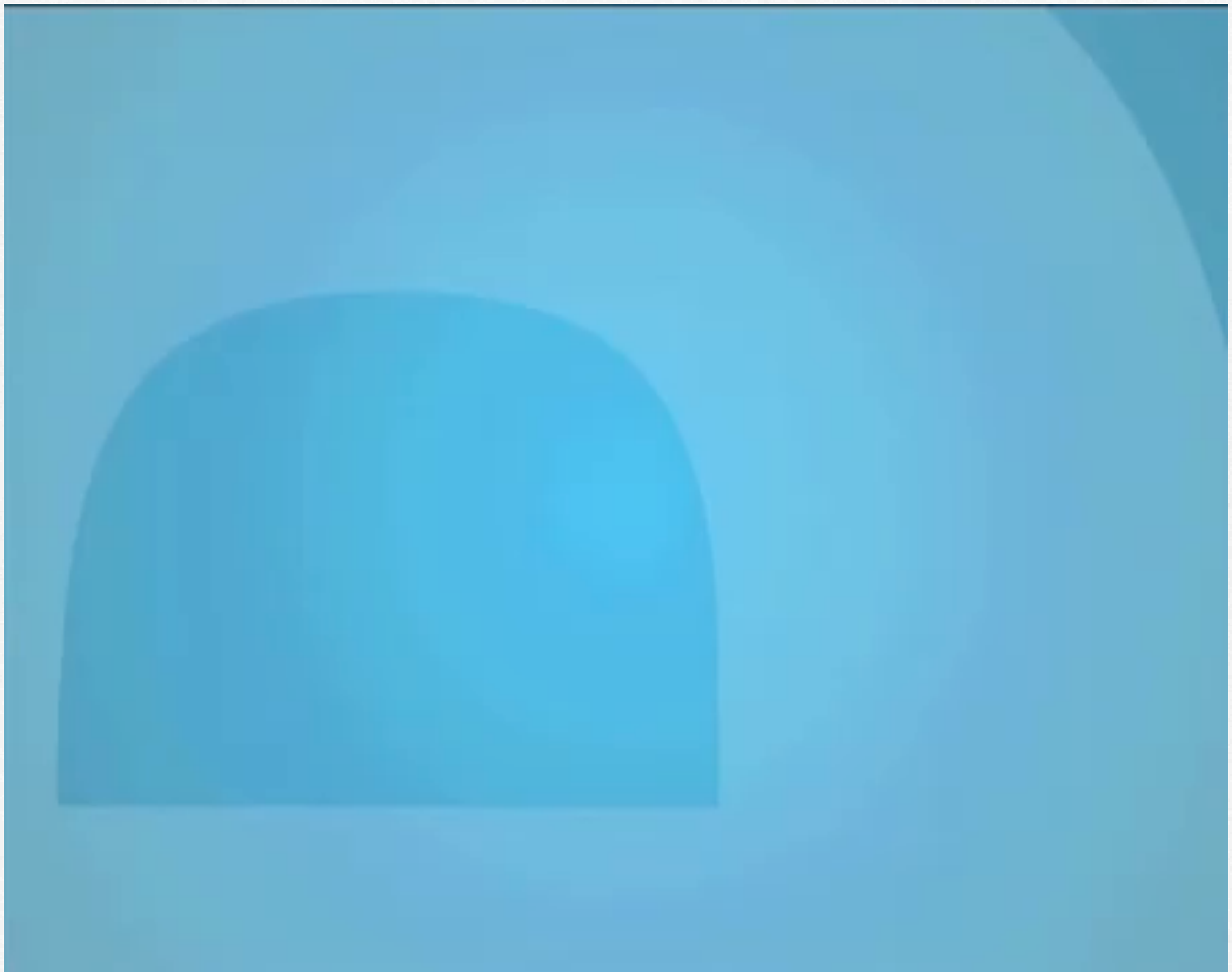

adhesion reduction